

---

## Research Paper

---

# Alternating Current (AC) Iontophoretic Transport across Human Epidermal Membrane: Effects of AC Frequency and Amplitude

Guang Yan,<sup>1</sup> Qingfang Xu,<sup>2</sup> Yuri G. Anissimov,<sup>3</sup> Jinsong Hao,<sup>2</sup> William I. Higuchi,<sup>1</sup> and S. Kevin Li<sup>1,2,4</sup>

Received May 5, 2007; accepted July 2, 2007; published online August 17, 2007

**Purpose.** As a continuing effort to understand the mechanisms of alternating current (AC) transdermal iontophoresis and the iontophoretic transport pathways in the stratum corneum (SC), the objectives of the present study were to determine the interplay of AC frequency, AC voltage, and iontophoretic transport of ionic and neutral permeants across human epidermal membrane (HEM) and use AC as a means to characterize the transport pathways.

**Materials and Methods.** Constant AC voltage iontophoresis experiments were conducted with HEM in 0.10 M tetraethyl ammonium pivalate (TEAP). AC frequencies ranging from 0.0001 to 25 Hz and AC applied voltages of 0.5 and 2.5 V were investigated. Tetraethyl ammonium (TEA) and arabinose (ARA) were the ionic and neutral model permeants, respectively. In data analysis, the logarithm of the permeability coefficients of HEM for the model permeants was plotted against the logarithm of the HEM electrical resistance for each AC condition.

**Results.** As expected, linear correlations between the logarithms of permeability coefficients and the logarithms of resistances of HEM were observed, and the permeability data were first normalized and then compared at the same HEM electrical resistance using these correlations. Transport enhancement of the ionic permeant was significantly larger than that of the neutral permeant during AC iontophoresis. The fluxes of the ionic permeant during AC iontophoresis of 2.5 V in the frequency range from 5 to 1,000 Hz were relatively constant and were approximately 4 times over those of passive transport. When the AC frequency decreased from 5 to 0.001 Hz at 2.5 V, flux enhancement increased to around 50 times over passive transport.

**Conclusion.** While the AC frequency for achieving the full effect of iontophoretic enhancement at low AC frequency was lower than anticipated, the frequency for approaching passive diffusion transport at high frequency was higher than expected from the HEM morphology. These observations are consistent with a transport model of multiple barriers in series and the previous hypothesis that the iontophoresis pathways across HEM under AC behave like a series of reservoirs interconnected by short pore pathways.

**KEY WORDS:** AC; human skin; iontophoresis; transdermal; transport.

## INTRODUCTION

Symmetric alternating current (AC) could enhance transdermal transport of both neutral and ionic permeants primarily by means of electrophoresis and/or electric field-induced membrane alteration (1–3), similar to the flux enhancing mechanisms of direct current (DC) iontophoresis. Compared to the electrophoresis and electric field-induced membrane alteration, the contribution of electroosmosis to AC flux enhancement is relatively small. For example, it has been shown that the permeability coefficients of human

epidermal membrane (HEM) for neutral permeants are inversely proportional to HEM electrical resistances during both passive and AC iontophoretic transport with the same proportionality constants (3,4), suggesting membrane alteration as the only flux-enhancing mechanism for the neutral permeants during moderate voltage AC iontophoresis at frequencies of  $\geq 12.5$  Hz. It was also shown that the flux enhancement of AC transdermal iontophoresis is generally lower than that of DC iontophoresis (5). However, previous studies of AC and pulsed current iontophoresis have suggested that these iontophoresis protocols can cause less skin irritation and sensation compared with DC (6). Unlike DC, AC iontophoresis also does not alter the electrochemical environment of the solution surrounding the electrodes (7). Such alteration may cause electrochemical burns on the skin during long iontophoresis application or when an inappropriate electrode design is used (8). Besides reducing the potential of electrochemical burns, it was also found that AC can control and maintain the electrical resistance of skin at a target level that reduces iontophoretic flux variability of

<sup>1</sup> Department of Pharmaceutics & Pharmaceutical Chemistry, University of Utah, Salt Lake City, Utah 84112, USA.

<sup>2</sup> Division of Pharmaceutical Sciences, College of Pharmacy, University of Cincinnati, 3225 Eden Avenue, Rm 136 HPB, Cincinnati, Ohio 45267, USA.

<sup>3</sup> School of Biomolecular and Physical Sciences, Griffith University, Nathan, Queensland 4111, Australia.

<sup>4</sup> To whom correspondence should be addressed. (e-mail: likv@uc.edu)

neutral permeants compared to that during conventional constant current DC iontophoresis (9,10).

In the past decade, our laboratory has been studying the mechanisms of AC iontophoretic transport across HEM. In a previous paper of modeling AC iontophoretic transport of ionic permeants with Nuclepore membranes, the interplay between ionic permeant fluxes, applied AC voltage, and AC frequency has been investigated (2). A multiple-layer barrier in series model was proposed. According to the AC transport model derived in this previous study, the flux vs frequency relationship can be divided into five regions. At low AC frequency, the fluxes approach one-half of the DC iontophoresis steady-state flux value. Away from this one-half DC plateau to higher AC frequency, the fluxes decrease and are not proportional to the applied AC voltage. With further increase in AC frequency, a flux vs frequency plateau was observed. At even higher AC frequency, passive transport becomes increasingly dominant and transport eventually becomes entirely passive diffusion controlled. Previous AC iontophoresis experiments of HEM (3) have shown flux enhancement of an ionic permeant with little or no AC frequency dependence at 50 and 1,000 Hz, which is consistent with the mid-frequency plateau region observed in this multiple-layer barrier in series model. However, the experimental data in this previous study were limited and a conclusion cannot be generalized. Only two AC frequencies (50 and 1,000 Hz) and electric field-altered HEM at 2.5 and 5 V were investigated. It would be important to further examine the AC flux vs AC frequency relationship in a wider AC frequency range to provide a complete picture and test the previous hypothesis. A lower electric field should also be studied to cover a wider range of electrical potential that could be encountered in transdermal iontophoresis applications. This new information would allow further understanding of the AC transdermal iontophoresis mechanisms, so AC iontophoresis can be adequately utilized in drug delivery.

Understanding the relationships between transdermal flux, AC frequency, and AC voltage during AC iontophoresis also allows the utilization of the AC frequency at which maximum transdermal flux enhancement occurs. Recent development in transdermal iontophoresis technology has brought a number of AC transdermal iontophoresis systems to the market such as Lectro Patch<sup>®</sup> (General Medical Co., CA) and GlucoWatch<sup>®</sup> G2<sup>™</sup> Biographer (Cygnus Inc., CA). For example, Lectro Patch<sup>®</sup> operates under AC at a frequency of between 0.0027 and 10 Hz for drug delivery (8). GlucoWatch<sup>®</sup> G2<sup>™</sup> Biographer utilizes an iontophoresis protocol that alters the polarity of a DC for 3 min each 10-min cycle (11). Other AC frequency protocols for glucose monitoring such as with polarity alternating every 2.5 min and 7.5 min (12,13) and AC frequencies from 1 kHz (14,15) to as high as 100 kHz (16) were also examined. It is generally believed that flux enhancement increases with decreasing AC frequency during AC iontophoresis and that AC iontophoresis of higher AC frequency could reduce skin irritation and sensation. However, the AC frequency-flux relationship in transdermal transport has not been systematically quantified. Particularly, an important question remains. What is the AC frequency that provides the maximum flux enhancement (i.e., AC flux enhancement reaching one-half of that of DC)? In

order to optimize AC iontophoretic transport in drug delivery and analyte extraction, this question should be addressed.

AC iontophoresis studies can also provide insights into the transport pathways of the stratum corneum (SC) in passive transport and during iontophoresis. For example, the effective length of the transport pathway in SC can be determined by model analyses of transport data during AC. The intrinsic barrier properties of HEM can be studied using AC iontophoresis of voltage below the threshold of electric field-induced HEM alteration (17). The iontophoretic pathways of AC-altered HEM can be investigated using AC iontophoresis of higher voltage. It was previously hypothesized that there exists different transport pathways for ionic and neutral permeants (3) and for neutral permeants under the low and high AC voltage conditions in HEM (18). AC iontophoresis can provide an excellent opportunity to characterize the effective length of the iontophoretic transport pathways in SC which would be difficult to achieve in other experimental settings. Such assessment of the iontophoretic transport pathways in HEM can be accomplished by the methodology established in the previous study (3).

The objective of the present study was to assess the effects of the AC voltage and AC frequency upon the fluxes of model neutral and ionic permeants across HEM and continue to build upon the database using the methodology developed in our laboratory. Symmetric square-wave AC of 0.0001 to 25 Hz and amplitude of 0.5 and 2.5 V were used. This AC frequency and voltage range covered a range that had not been previously studied. The iontophoretic transport pathways in AC-altered HEM (newly induced pathways) and those related to the intrinsic properties of HEM (pre-existing pathways) were examined in the 2.5 and 0.5 V AC experiments, respectively. Flux enhancement due to electroosmosis and that of electrophoresis was studied with the neutral permeant ARA and charged permeant TEA. The data were interpreted using the models developed based on the Nernst-Planck theory in previous studies (2,3,19), and the effective length of the iontophoretic transport pathway were determined. AC frequency for maximum AC iontophoretic flux enhancement was identified. AC flux data of 50 and 1,000 Hz and 2.5 V from a previous study (3) were also included in the present model analysis.

## EXPERIMENTAL SECTION

### Materials

Radiolabeled [<sup>14</sup>C] tetraethyl ammonium (TEA) bromide was purchased from PerkinElmer Life Sciences, Inc. (Boston, MA). [<sup>3</sup>H] arabinose (ARA) was purchased from Moravak Biochemical (Brea, CA). Millipore GVWP filter membranes were purchased from Millipore Corporation (Bedford, MA). Tetraethyl ammonium hydroxide (20%, w/w) and pivalic acid were purchased from Sigma Chemicals (St. Louis, MO). 0.1 M tetraethyl ammonium pivalate (TEAP) solution was prepared by mixing approximately equal quantities of tetraethyl ammonium hydroxide and pivalic acid in deionized water and the solution was adjusted to pH 7.4 by further adding pivalic acid or TEA hydroxide.

Phosphate buffered saline (PBS) of 0.1 M ionic strength and pH 7.4 was prepared by reagent grade chemicals.

### HEM Selection

Human epidermal membrane (HEM) was prepared by heat separation of human cadaver skin obtained from skin bank and mounted on side-by-side diffusion cells as described previously (20). Briefly, a backing Millipore membrane was placed on the dermis side of HEM. The HEM and Millipore membrane were mounted together between two side-by-side diffusion half-cells with the SC side facing the donor chamber. The diffusion cells had diffusion surface area of around  $0.74 \pm 0.05 \text{ cm}^2$  and cell volume of 2.5 ml. HEM was equilibrated with 0.1 M PBS overnight in a  $37 \pm 1^\circ\text{C}$  waterbath. A four-electrode potentiostat system (JAS Instrument System, Inc., Salt Lake City, UT) or a waveform generator (Model 33220A, Agilent Technologies, Santa Clara, CA) was used to measure the electrical resistance of HEM using Ohm's law (21). Only HEM samples with initial resistance greater than  $\approx 10 \text{ k}\Omega \text{ cm}^2$  were used in the present study.

### Experimental Setup and Single Stage Experiments

After the overnight equilibration, the PBS solution in the side-by-side diffusion cell was withdrawn, both chambers were washed with 0.1 M TEAP solution one time, and then both were filled with 2 ml 0.1 M TEAP solution. Passive permeation and AC iontophoresis experiments were performed in the side-by-side diffusion cell system (3). Symmetric square-wave AC iontophoresis of two different amplitudes (0.5 and 2.5 V, bipolar) and seven different frequencies (0.0001, 0.001, 0.01, 0.125, 0.5, 5, and 25 Hz) was investigated. Three different types of AC power sources were used to provide square-wave AC across the HEM for the studies: 0.0001, 0.001, and 0.01 Hz, Agilent Technologies Model 33220A waveform generator (Santa Clara, CA), 0.125 and 0.5 Hz, JAS Instrument System Model JJ 1276 waveform programmer (Salt Lake City, UT), and 5 and 25 Hz, BK precision Model 4011 function generator (Placentia, CA). [ $^{14}\text{C}$ ] TEA and [ $^3\text{H}$ ] ARA were the permeants. Ag/AgCl strips and platinum wires (0.5 mm diameter and 3 cm length) were used as the driving electrodes for the AC electric field in the experiments of 0.0001 to 0.01 Hz and 0.125 to 25 Hz, respectively. A fixed reference resistor was connected in series with the diffusion cell system in the electric circuit. The AC voltage across HEM and the AC voltage across the fixed resistor were monitored by an oscilloscope (Tektronix Model 2211, Beaverton, OR) and/or multimeters (Fluke 73III, Everett, WA). The skin electrical resistance was calculated based on Ohm's law. AC amplitude across the skin was maintained constant by manually adjusting the output AC voltage of the waveform programmer. When HEM electrical resistance becomes relatively stable (generally within 30 min into the iontophoresis experiments), trace amounts of radiolabeled TEA and ARA were introduced into the donor chamber. The final specific activities of [ $^{14}\text{C}$ ] TEA and [ $^3\text{H}$ ] ARA in the donor solution were approximately  $0.2\text{--}1 \times 10^7 \text{ dpm/ml}$ . The duration of the transport experiments was approximately 6 h under the AC condition. During iontophoresis, the whole 2 ml were taken from the receiver

chamber every 1 h as samples and replaced with 2 ml fresh TEAP solution. Ten-microliter samples were withdrawn from the donor every 2 h. The samples were mixed with 10 ml of scintillation cocktail (Ultima Gold<sup>TM</sup>, PerkinElmer Life Sciences, Meriden, CT) and assayed by a liquid scintillation analyzer (Packard TriCarb<sup>TM</sup> model 1900TR or Beckman model LS6500). The flux ( $J$ ) and permeability coefficient ( $P$ ) of the permeant transported across the membrane were calculated at steady-state under sink conditions:

$$J = \frac{1}{A_D} \frac{\Delta Q}{\Delta t} \quad (1)$$

$$P = \frac{1}{C_D A_D} \frac{\Delta Q}{\Delta t} \quad (2)$$

where  $C_D$  is the concentration of the permeant in the donor chamber,  $A_D$  is the diffusional surface area,  $\Delta Q/\Delta t$  is the slope of the cumulative amount of the permeant transported across the membrane into the receiver chamber vs time plot.

### Multiple Stage Experiments

In selected AC experiments, such as those of the 0.5 V AC protocol, passive and AC transport experiments were carried out with the same HEM samples. These experiments were divided into either two or three stages. In the three-stage experiments, stage I was a passive transport experiment. Stage II was AC iontophoresis experiment on the same membrane. Stage III was a repeat of the passive experiment of stage I after stage II. Stages I and III were the controls in data analyses to minimize the effects of skin-to-skin variability. In the two-stage experiments, stage III was not carried out.

### Test of AC Waveform Symmetry from the Power Source

The AC waveform provided by the power supply might not be perfectly symmetric. It was noted that a few hundredth of a voltage differential between the positive and negative output from the power source (or a few percent of the total area under the waveforms) could induce significant errors in the present study. In the experiments of AC frequency higher than 20 Hz, the voltage across HEM was monitored by a DC voltmeter and a small DC offset was applied if necessary to ensure that there was no net DC across the HEM during AC iontophoresis. At lower AC frequency, the voltmeter reading fluctuated between the two AC polarities and monitoring the net DC across HEM during AC iontophoresis with a DC voltmeter became difficult. In this case, the leads of the power output were switched (reversed) in the middle of selected iontophoresis experiments. The permeability coefficient in the first part of the iontophoresis run (before switching) was compared with that in the second part of the iontophoresis run (after switching).

### Theory and Model Analysis

The flux during iontophoresis can be described by the Nernst–Planck equation (22) modified by hindered transport theory (23). For DC iontophoresis of a charged permeant, the enhancement factor ( $E_{\Delta\psi}$ ), the ratio of iontophoretic flux over passive flux at the same donor concentration and same membrane electrical resistance, under the condition when the molecular size of permeant is the same as those of the background electrolyte (23) can be expressed as:

$$E_{\Delta\psi} = \frac{Pe + K}{1 - \exp(-K - Pe)} \quad (3)$$

where  $Pe$  is the Peclet number that characterizes the effect of convective solvent flow and  $K = zF(\Delta\psi)/(R_{gas}T)$ , in which  $\Delta\psi$  is the applied voltage across the membrane,  $F$  is the Faraday constant,  $R_{gas}$  is the gas constant,  $T$  is the temperature, and  $z$  is the charge number of the permeant (3). For DC iontophoresis transport at 37°C when the applied electric field across the membrane is 1 V,  $K=37$ . For a neutral permeant, the enhancement factor ( $E_{\Delta\psi}$ ) becomes:

$$E_{\Delta\psi} = \frac{Pe}{1 - \exp(-Pe)} \quad (4)$$

Transdermal flux enhancement due to electroosmosis during DC iontophoresis is generally less than 20% of that of electrophoresis for a small permeant (19,23), and the average value of  $Pe$  is approximately one-tenth of the  $K$  value. From Eqs. 3 and 4,  $E_{\Delta\psi} \approx 20$  and 104 for TEA and 2 and 10 for ARA at 0.5 and 2.5 V DC iontophoresis, respectively.

For AC iontophoresis, a previously described homogeneous membrane model (19) was used as a first approximation in analyzing AC flux data. This model assumes Nernst–Planck flux behavior with time variable electric potential. It has to be noted that this assumption is only valid if membrane properties are not altered due to the electric field. In the present notation the approximate equation for the flux enhancement due to AC iontophoresis of square waveform is:

$$E_{\Delta\psi AC} = \frac{1 + 0.18\sqrt{K/\varphi^3}}{1 + 1.4\sqrt{K/\varphi^{14}}} + \frac{K}{2(1 + 0.25\varphi^{10})(1 + \varphi + 0.2K^{0.7}\varphi^3)} \quad (5)$$

where  $\varphi = \frac{f}{f^*} = \frac{2f\Delta x^2}{KD_{eff}}$ ,  $f$  is the frequency of the AC,  $\Delta x$  is the effective membrane thickness, and  $D_{eff}$  is the effective diffusion coefficient in the membrane ( $D_{eff}=HD$ ), where  $H$  is the hindrance factor of diffusion and iontophoretic transport and  $D$  is the diffusion coefficient for the permeant.  $f^*$  is defined as the characteristic frequency, in which  $0.5/f^*$  is related to the time for an ion to transport across the entire membrane barrier in one-half cycle. Note that for low frequencies  $\varphi < 1$ ,  $E_{\Delta\psi AC} \approx K/2$ , i.e., the low frequency AC iontophoresis produces half the enhancement of corresponding DC iontophoresis.

The effective length of the permeation pathway of HEM (or effective thickness,  $\Delta x$ ) during AC iontophoresis was determined with the homogenous membrane model (Eq. 5) and compared with the physical parameters of SC.

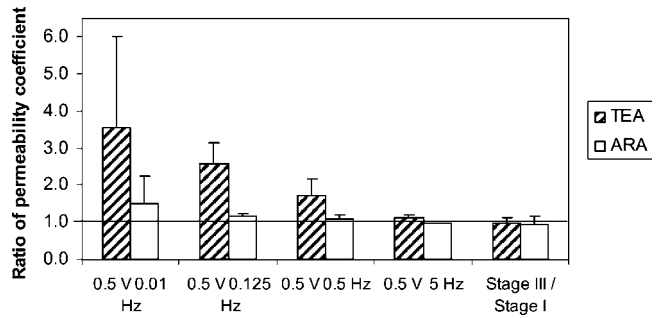


**Fig. 1.** The ratios of the permeability coefficients of TEA and ARA during 0.5 V AC iontophoresis in stage II to those of passive transport before iontophoresis in stage I in the multiple-stage iontophoresis study and ratios of the permeability coefficients of passive transport for TEA and ARA in stage III after iontophoresis to those in stage I before iontophoresis.

## RESULTS

### Multiple Stage Experiments

Figure 1 presents the ratios of the permeability coefficients of stage II to stage I under the AC conditions of 0.5 V and 0.01 to 5 Hz. There was no considerable flux enhancement for the neutral permeant ARA due to the AC electric fields studied in the present study. The highest permeability coefficients observed for ARA in stage II under the 0.01 Hz AC condition were around an average of 1.5-fold higher than those in stage I passive transport but show no statistical differences compared to stage I ( $p=0.1$ ,  $t$  test). For the positively charged permeant TEA, there was no significant flux enhancement at 5 Hz AC. Flux enhancement was observed when the AC frequency decreased from 5 to 0.01 Hz ( $p<0.02$ ,  $t$  tests). From 0.5 to 0.01 Hz, TEA fluxes increased to approximately 3 times of the passive fluxes. Figure 1 also presents the ratios of the passive permeability coefficients in stage III to those in stage I. These permeability coefficient ratios are close to unity, suggesting that AC of 0.5 V did not cause any significant alterations to the HEM barrier. This is consistent with the conclusion in a previous study that electric field of  $\approx 0.5$  V or less does not significantly alter the HEM barrier during iontophoresis (17).

### Permeability and Resistance Correlation

The logarithms of the steady-state permeability coefficients ( $P$ ) were plotted against the logarithms of the HEM electrical resistances ( $R$ ) of the transport for TEA and ARA in Figs. 2 and 3, respectively. The data from a previous 50 and 1,000 Hz AC transport study (3) are also presented in the figures for comparison. The passive transport data in the previous study were combined with those in the present study and served as the baseline. These figures show good correlations between HEM permeability coefficient and HEM electrical resistance under the passive and AC conditions, with the  $\log P$  vs  $\log R$  linear correlations providing slopes of approximately  $-1$ . This relationship is consistent with the transport theory when the background electrolytes and the permeants have similar molecular sizes.

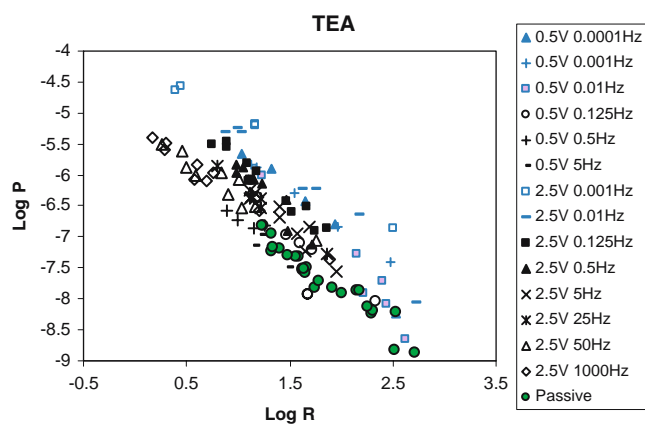


**Fig. 2.** Relationship between TEA permeability coefficient of HEM and HEM electrical resistance during AC iontophoresis of 0.5 and 2.5 V at 0.0001 to 1000 Hz. Data of 2.5 V at 50 and 1000 Hz were obtained from Yan *et al.* (3). Permeability coefficient,  $P$ , is in cm/s; electrical resistance,  $R$ , is in k $\Omega$ .

As discussed in previous studies (3,4,23), when the permeants and the background electrolyte have similar molecular sizes, these ions experience the same hindrance effect through the pore pathway in HEM. The electrical resistance is therefore closely correlated to the fluxes of the permeants. This allows the approach of using the  $\log P$  vs  $\log R$  relationship to determine AC flux enhancement in the present study.

### Test of AC Waveform Symmetry

In the experiments to test for AC waveform symmetry, the leads of the power output were switched (reversed) in the middle of an iontophoresis run. The permeability coefficients in the first part of the iontophoresis run (before switching) were found to be generally within 25% of those in the second part of the iontophoresis run (after switching). In three extreme cases, they were still within 40% of each other. Although this would create some uncertainties under the experimental conditions in the AC studies, waveform asymmetry was random error and should not affect the conclusion in the present study.

### Effects of Frequency upon Flux Enhancement

Tables I and II summarize the y-intercept values of the  $\log P$  vs  $\log R$  plots for TEA and ARA transport under different AC frequency and voltage conditions in Figs. 2 and 3. Flux enhancement due to the AC electric field was calculated by comparing the permeability coefficients of the ionic and neutral permeants under the AC iontophoresis conditions and those under passive conditions at the same HEM electrical resistance (differential in  $\log P$  values at the same  $\log R$ ). This was accomplished by using the permeability vs electrical resistance relationship during passive and iontophoretic transport, respectively (3):

$$\log P_{\text{passive}} = -\log R + B_p \quad (6)$$

$$\log P_{\Delta y} = -\log R + B_i \quad (7)$$

Flux enhancement factors for the TEA and ARA were calculated by the difference between the y-intercepts  $B_p$  and  $B_i$  of the regression lines in Figs. 2 and 3 for TEA and ARA, respectively. The enhancement factors of TEA and ARA calculated with this method are summarized in Tables I and II.

Figure 4 shows the relationship between the enhancement factor due to AC iontophoresis and the AC frequency. Note that membrane porosity and other HEM barrier parameters were factored out in the analysis using Eqs. 6 and 7, this technique thus accounting for flux enhancement due to electric field-induced membrane alteration as well (3). Therefore, the enhancement factor presented in the figure was the enhancement primarily due to electrophoresis and electroosmosis. According to the ARA data, there was no observable flux enhancement due to electroosmosis at AC frequencies greater than 0.125 Hz under AC electric fields used in the present study. At lower AC frequencies, flux enhancement of ARA during AC approached approximately one-eighth and one-thirtieth of that of TEA during DC at 0.5 and 2.5 V, respectively. For TEA, under the 0.5 V AC conditions, no enhancement due to electrophoresis and electroosmosis was observed at AC frequencies greater than 0.5 Hz; when the AC frequency decreased from 0.5 to 0.0001 Hz, an approximately tenfold flux enhancement over passive transport was observed. This enhancement value was approximately one-half of the DC iontophoresis flux enhancement in each flux enhancing AC half cycle). Under the 2.5 V AC conditions, flux enhancement over passive transport was around three to fourfold in the frequency range 5 to 1,000 Hz. As the AC frequency decreased from 5 to 0.001 Hz, the enhancement factor increased to 49, which was approximately one-half of the DC iontophoresis flux enhancement at 2.5 V.

### Model Analysis of the TEA Results

Figure 5 shows the fit of the homogenous membrane model to the TEA experimental data obtained during 0.5 and

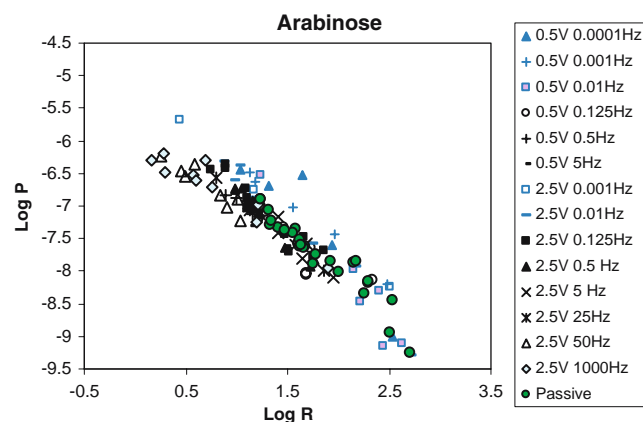


**Fig. 3.** Relationship between ARA permeability coefficient of HEM and HEM electrical resistance during AC iontophoresis of 0.5 and 2.5 V at 0.0001 to 1000 Hz. Data of 2.5 V at 50 and 1,000 Hz were obtained from Yan *et al.* (3). Permeability coefficient,  $P$ , is in cm/s; electrical resistance,  $R$ , is in k $\Omega$ .

**Table I.** Summary of the Data in the log *P* vs log *R* Plot for TEA

AC Amplitude (V)	AC Frequency (Hz)	y-Intercept <sup>a</sup>	Enhancement Factor
Passive <sup>b</sup>	–	–5.84±0.04	–
0.5	0.0001	–4.8±0.2	10
0.5	0.001	–4.77±0.05	12
0.5	0.01	–5.4±0.2	3
0.5	0.125	–5.7±0.2	1.2
0.5	0.5	–5.67±0.04	1.5
0.5	5	–5.91±0.07	0.8
2.5	0.001	–4.14±0.06	49
2.5	0.01	–4.48±0.12	23
2.5	0.125	–4.85±0.05	10
2.5	0.5	–4.99±0.06	7
2.5	5	–5.27±0.07	4
2.5	25	–5.25±0.05	4
2.5	50	–5.29±0.05 <sup>c</sup>	3
2.5	1000	–5.30±0.04 <sup>c</sup>	3

<sup>a</sup> y-Intercept and its SD were calculated from the linear least squares regression using Eqs. 6 and 7.

<sup>b</sup> Determined by combining the data from the present study and Yan *et al.* (3).

<sup>c</sup> Raw data were obtained from Yan *et al.* (3) to generate the linear least squares regression and compare with new passive data.

2.5 V AC iontophoresis. Within experimental error, the 0.5 V data can be adequately described by the homogenous membrane model. The  $f^*$  value of the fit using the 0.5 V data is 0.01 Hz, corresponding to effective thickness of 0.3 mm assuming that the effective diffusion coefficient of TEA in the SC pathway is  $10^{-6}$  cm<sup>2</sup>/s. Unlike the satisfactory fit for the 0.5 V data, the fit for the 2.5 V data is poor. Figure 6 presents the effective membrane thickness (the length of the transport pathway) calculated using the homogeneous membrane model (Eq. 5) and the experimental enhancement factors at AC frequencies from 0.01 to 1,000 Hz. The bars in the figure represent the range of membrane thicknesses calculated with the assumption of TEA diffusion coefficients of  $3 \times 10^{-7}$  to  $4 \times 10^{-6}$  cm<sup>2</sup>/s. This range covers the diffusion coefficients of the permeant in significantly hindered to slightly hindered transport that is typical in passive and iontophoretic transport across HEM (4,21). Within the frequency range presented in the figure, the calculated effective thickness ranges from

approximately 2 to 800  $\mu$ m (from frequency of 1,000 to 0.01 Hz, respectively). This range is more than 2 orders of magnitude greater than the thickness values of fully hydrated HEM and SC (approximately 20–70  $\mu$ m, unpublished data). This highly variable calculated membrane thickness is again evidence of the poor agreement of the homogenous membrane model for the TEA iontophoretic transport at 2.5 V.

## DISCUSSION

An important finding in the present study is the relationship between flux enhancement and AC frequency for iontophoretic transport across hydrated HEM. These results provide insights into the transport characteristics of fully hydrated HEM during iontophoresis. In Fig. 4, while the 0.5 V AC experiments likely provide information regarding the properties of the intrinsic iontophoretic transport pathways in HEM, the results of 2.5 V AC iontophoresis appear

**Table II.** Summary of the Data in the log *P* vs log *R* Plot for ARA

AC Amplitude (V)	AC Frequency (Hz)	y-Intercept <sup>a</sup>	Enhancement Factor
Passive <sup>b</sup>	–	–5.91±0.05	–
0.5	0.0001	–5.5±0.3	3
0.5	0.001	–5.47±0.06	2.8
0.5	0.01	–6.0±0.2	0.9
0.5	0.125	–6.0±0.1	0.8
0.5	0.5	–5.92±0.03	1.0
0.5	5	–6.04±0.07	0.8
2.5	0.001	–5.50±0.12	3
2.5	0.01	–5.69±0.14	2
2.5	0.125	–5.78±0.06	1.4
2.5	0.5	–5.85±0.06	1.2
2.5	5	–5.95±0.05	0.9
2.5	25	–5.92±0.05	1.0
2.5	50	–5.98±0.05 <sup>c</sup>	0.8
2.5	1000	–5.96±0.06 <sup>c</sup>	0.9

<sup>a</sup> y-Intercept and its SD were calculated from the linear least squares regression using Eqs. 6 and 7.

<sup>b</sup> Determined by combining the data from the present study and Yan *et al.* (3).

<sup>c</sup> Raw data were obtained from Yan *et al.* (3) to generate the linear least squares regression and compare with new passive data.

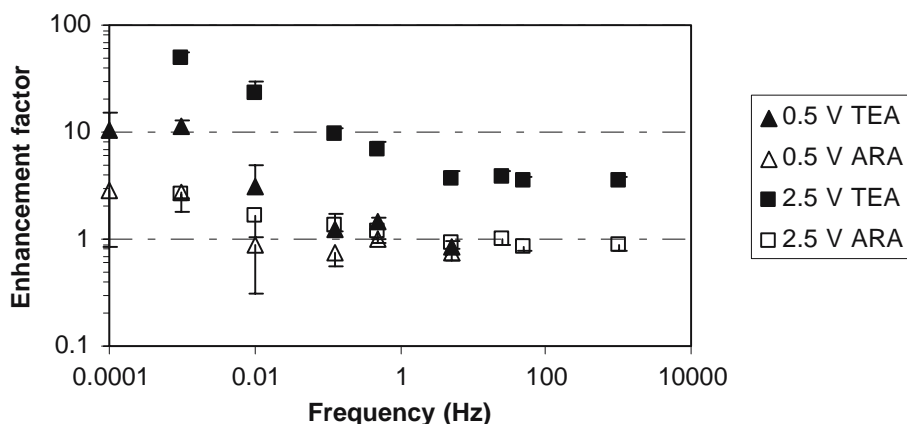


**Fig. 4.** Enhancement factors for transdermal transport of TEA and ARA at AC frequencies from 0.0001 to 1000 Hz during AC iontophoresis at 0.5 and 2.5 V. Enhancement factors of 2.5 V at 50 and 1,000 Hz were calculated from data obtained from Yan *et al.* (3).

to be related to the properties of the HEM involving pathways induced during iontophoresis. The AC flux enhancement vs AC frequency profile at 0.5 V is generally consistent with the homogenous model. The model-calculated long effective length (0.3 mm) may be viewed as being consistent with the complex pre-existing intercellular pore structure of the SC. At 2.5 V AC, the TEA enhancement vs

frequency plot suggests that the homogeneous barrier model is inadequate. The shape of the TEA AC flux enhancement vs AC frequency profile at 2.5 V is similar to those of previous model simulation with synthetic Nuclepore membranes (2). In this previous simulation study, which involved a model of multiple barriers with water reservoirs in series, the relationship of TEA flux vs AC frequency under a constant electric field could be divided into five main regions as pointed out in the Introduction. At the high AC frequency extreme, the flux approached the passive permeability limit. At the low AC frequency extreme, the flux approached the upper limit of permeability corresponding to one-half of the expected permeability for DC iontophoresis; when the half cycle time period is significantly larger than the transport lag time, the square-wave AC field is essentially acting as 50% of a DC field to enhancing transport. In the middle region between these two extremes, a constant flux relatively independent of frequency was observed. This middle region is the main difference between a homogenous barrier model and the multiple-barrier model. The present AC enhancement data for TEA obtained at 2.5 V appear to demonstrate this multi-region behavior.

Although a homogenous membrane model does not explain all aspects of the 2.5 V experimental data, such a model (19) is still useful in the analysis of the SC iontopho-

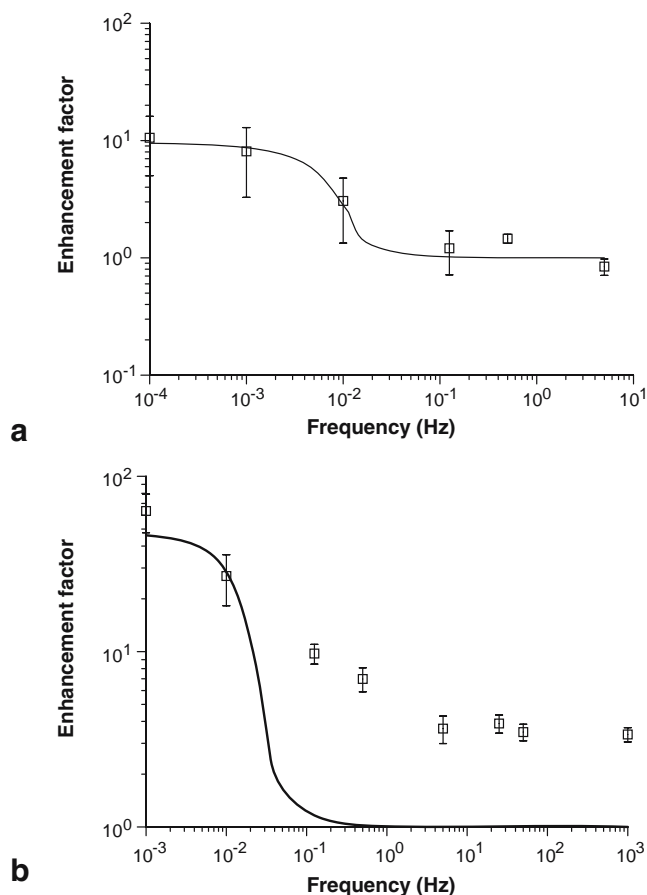


**Fig. 5.** Fit of the homogeneous membrane model to the data on the relationship between TEA iontophoretic transport enhancement and AC frequency during **a** 0.5 V and **b** 2.5 V AC iontophoresis.

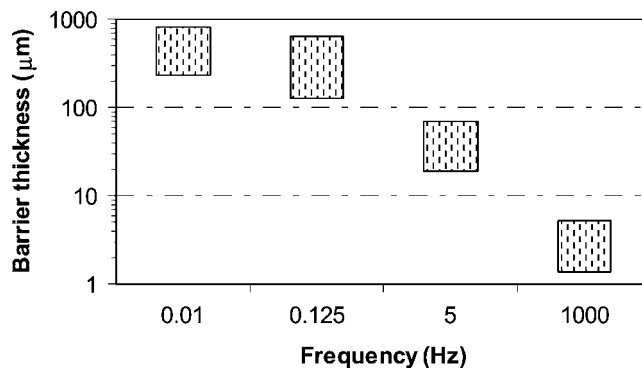


**Fig. 6.** Effective barrier thicknesses calculated using the homogeneous membrane model and the enhancement factor data at 2.5 V and AC frequencies from 0.01 to 1,000 Hz. The bars represent the ranges calculated from the assumption that the diffusion coefficient of TEA in the SC pathway is  $3 \times 10^{-7}$  and  $4 \times 10^{-6}$  cm<sup>2</sup>/s.

resis transport pathway situation as a heterogeneous membrane might be viewed as a combination of two or more pathways in series and/or in parallel. In the 2.5 V AC study, the enhancement factors of 23 and 49 for TEA at 0.01 and 0.001 Hz, respectively, would suggest long transport pathway length (thickness) barriers in HEM SC. The effective length of the transport pathway estimated using the homogenous model was 0.4 mm when the diffusion coefficient of TEA was assumed to be  $10^{-6}$  cm<sup>2</sup>/s. This would suggest that the skin appendages are not the dominant iontophoresis pathway because thickness based on skin appendages across SC is expected to be an order of magnitude smaller than 0.4 mm (24). Further, this latter thickness value is greater than the length of the SC intercellular pathways (0.06 mm) using the tortuosity value derived from the SC morphology (25), suggesting permeant-to-SC binding or permeant loading into and out of reservoir-like structures in the SC may be important. At the other end of the frequency spectrum in Fig. 4, different from the low AC frequency situation, the threefold flux enhancement at 1,000 Hz would suggest a very short iontophoresis transport pathway. The effective length calculated for such a transport pathway would be shorter than the physical thickness of HEM SC (less than 10  $\mu$ m) and might be considered unreasonable. Unfortunately, meaningful higher frequency AC experiments cannot be easily conducted to further investigate the iontophoresis pathway question due to the interference of skin electrical capacitance in the diffusion cell system (resulting in difficulties in controlling the voltage and the AC waveforms across HEM) and other equipment limitations. Nonetheless, the above analysis suggests that a homogenous membrane model does not adequately describe SC iontophoretic transport and a multiple barrier heterogeneous SC model is likely necessary to account for the experimental data at 2.5 V.

One possible explanation of the deviation of the 2.5 V experimental data from the homogenous membrane model is a distribution of pore lengths of the SC transport pathways during iontophoresis (rather than a single dominant pathway). To fit the experimental data, a distribution of pore lengths more than 2 orders of magnitude is required. Such pore length distributions might be rationalized on the basis of iontophoretic transport involving both the intercellular pathways and the skin appendages. Transport pathways resulting from electroporation at the appendages might also be important (24). However, this probably cannot explain the pathway length of <10  $\mu$ m calculated from the flux enhancement data at 1,000 Hz assuming a diffusion coefficient in the pore of  $\sim 10^{-6}$  cm<sup>2</sup>/s. A second possible explanation for this short path length is that the SC pore pathways may be interrupted by pools of water that can be described as a collection of thin barriers with water reservoirs in-between. This multi-barrier heterogeneous SC model is supported by the observation of water reservoirs in the SC intercellular space after skin hydration (26,27), in which the interconnected aqueous reservoirs become part of the barrier structure in fully hydrated HEM (3). Another possible explanation is that the homogenous membrane model is not applicable for the case when intrinsic membrane properties are altered due to transmembrane electrical potential (19), and therefore does not adequately describe AC iontophoresis at 2.5 V. Transdermal iontophoretic transport could deviate from the homogenous membrane

model at 2.5 V due to the latter two explanations alone or a combination of all three explanations. It is clear from the present study that the iontophoretic transport pathways at 2.5 V, which can involve electric field induced-pores, can be more complicated than the conventional mechanism of iontophoretic transport across either the appendages or intercellular pathways.

No or little enhancement due to electroosmosis was observed at AC frequency  $\geq 0.5$  Hz at 0.5 and 2.5 V. This is consistent with previous findings that AC iontophoresis at moderate frequencies does not enhance the transport of neutral permeants (3,4). Previous studies have shown that flux enhancement due to electroosmosis is generally less than 20% (average of around 10%) of that due to electrophoresis for small permeants (23). The ARA data in the present study fall in this 5 to 20% range. According to the TEA and ARA results in Fig. 4, flux enhancement due to electroosmosis at 0.5 V is approximately 20% of the total electrotransport enhancement at the low frequency plateau, and the contribution of electroosmosis to total electrotransport at 2.5 V is approximately 5% in the same frequency region. In addition, flux enhancement at 0.5 V and 0.001 Hz is essentially the same as that at 2.5 V and 0.001 Hz for ARA. The decrease in electroosmosis contribution from 0.5 to 2.5 V suggests different pore charge densities between the electric field-induced pores and the pre-existing pores in SC. These results are consistent with a previous finding (18).

It should be noted that the voltage conditions (0.5 and 2.5 V) used in the present study cover the voltage range commonly encountered in transdermal iontophoretic transport in human in practice: the applied voltage across skin ranges from 0.4 V to 3 V when the skin electrical resistance is 4 to 10 k $\Omega$ cm<sup>2</sup> under the current density of 0.1 or 0.3 mA/cm<sup>2</sup>. The fully hydrated SC condition is also likely to be encountered *in vivo* under prolonged skin exposure to a transdermal iontophoresis electrode. Under these conditions, very low frequency is required to provide the maximum flux enhancement in AC transdermal iontophoresis. AC flux enhancement reaches the maximum value (of one-half of the DC flux enhancement) at 0.001 Hz under the applied electric fields examined in the present study. This is consistent with previous AC studies conducted at AC frequency much higher than this maximum region showing significantly larger DC flux enhancement than that of AC (5). To put this observation into a practical perspective, maximum AC flux enhancement is achieved at frequency at or below 0.001 Hz, this corresponding to 8.3 min of DC in each direction in an AC cycle. The AC frequencies used in the commercial AC transdermal iontophoresis devices such as the Lectro Patch<sup>®</sup> (General Medical Co., CA), GlucoWatch<sup>®</sup> G2<sup>™</sup> Biographer (Cygnus Inc., CA) are barely in this frequency range. The low frequency required to reach the maximum AC flux enhancement is unexpected as one would predict that the thin SC would require less than 1 min to achieve full iontophoresis enhancement effect in transdermal transport. This illustrates the importance of understanding the AC flux enhancement-AC frequency relationships to provide information for future development of AC iontophoretic delivery so that the enhancement effects of electrophoresis and electroosmosis in transdermal iontophoretic transport involving alternating polarity can be optimized. Future studies are required to determine the AC flux vs AC frequency



relationships under different conditions such as in phosphate buffered saline (vs in TEAP) for iontophoretic extraction and in drug solutions for delivery.

## ACKNOWLEDGMENTS

This research was supported by NIH Grant GM 063559. The authors thank Watson Pharmaceuticals Inc. (Salt Lake City, UT) for their generous donation of some of the HEM samples used in the present study and Dr. Michael S. Roberts for his helpful discussion.

## REFERENCES

1. Y. Song, S. K. Li, K. D. Peck, H. Zhu, A. H. Ghanem, and W. I. Higuchi. Human epidermal membrane constant conductance iontophoresis: alternating current to obtain reproducible enhanced permeation and reduced lag times of a nonionic polar permeant. *Int. J. Pharm.* **232**:45–57 (2002).
2. G. Yan, S. K. Li, K. D. Peck, H. Zhu, and W. I. Higuchi. Quantitative study of electrophoretic and electroosmotic enhancement during alternating current iontophoresis across synthetic membranes. *J. Pharm. Sci.* **93**:2895–2908 (2004).
3. G. Yan, K. D. Peck, H. Zhu, W. I. Higuchi, and S. K. Li. Effects of electrophoresis and electroosmosis during alternating current iontophoresis across human epidermal membrane. *J. Pharm. Sci.* **94**:547–558 (2005).
4. S. K. Li, A. H. Ghanem, K. D. Peck, and W. I. Higuchi. Pore induction in human epidermal membrane during low to moderate voltage iontophoresis: a study using AC iontophoresis. *J. Pharm. Sci.* **88**:419–427 (1999).
5. G. Yan, S. K. Li, and W. I. Higuchi. Evaluation of constant current alternating current iontophoresis for transdermal drug delivery. *J. Control. Release* **110**:141–150 (2005).
6. K. Okabe, H. Yamaguchi, and Y. Kawai. New iontophoretic transdermal administration of the beta-blocker metoprolol. *J. Control. Release* **4**:79–85 (1986).
7. J. P. Howard, T. R. Drake, and D. L. Kellogg. Effect of alternating current iontophoresis on drug delivery. *Arch. Phys. Med. Rehabil.* **76**:463–466 (1995).
8. R. Tapper. Iontophoretic treatment system. U.S. Patent 5,224,927, July 6, 1993.
9. H. Zhu, S. K. Li, K. D. Peck, D. J. Miller, and W. I. Higuchi. Improvement on conventional constant current DC iontophoresis: a study using constant conductance AC iontophoresis. *J. Control. Release* **82**:249–261 (2002).
10. H. Zhu, K. D. Peck, D. J. Miller, M. R. Liddell, G. Yan, W. I. Higuchi, and S. K. Li. Investigation of properties of human epidermal membrane under constant conductance alternating current iontophoresis. *J. Control. Release* **89**:31–46 (2003).
11. R. O. Potts, J. A. Tamada, and M. J. Tierney. Glucose monitoring by reverse iontophoresis. *Diabetes Metab. Res. Rev.* **18** (Suppl 1) S49–S53 (2002).
12. J. A. Tamada, N. J. Bohannon, and R. O. Potts. Measurement of glucose in diabetic subjects using noninvasive transdermal extraction. *Nat. Med.* **1**:1198–1201 (1995).
13. J. A. Tamada and K. Comyns. Effect of formulation factors on electroosmotic glucose transport through human skin *in vivo*. *J. Pharm. Sci.* **94**:1839–1849 (2005).
14. S. K. Li, W. I. Higuchi, H. Zhu, S. E. Kern, D. J. Miller, and M. S. Hastings. *In vitro* and *in vivo* comparisons of constant resistance AC iontophoresis and DC iontophoresis. *J. Control. Release* **91**:327–343 (2003).
15. H. Haga, T. Shibaji, and M. Umino. Lidocaine transport through living rat skin using alternating current. *Med. Biol. Eng. Comput.* **43**:622–629 (2005).
16. T. Kinoshita, T. Shibaji, and M. Umino. Transdermal delivery of lidocaine *in vitro* by alternating current. *J. Med. Dent. Sci.* **50**:71–77 (2003).
17. H. Inada, A. H. Ghanem, and W. I. Higuchi. Studies on the effects of applied voltage and duration on human epidermal membrane alteration/recovery and the resultant effects upon iontophoresis. *Pharm. Res.* **11**:687–697 (1994).
18. S. K. Li, A. H. Ghanem, and W. I. Higuchi. Pore charge distribution considerations in human epidermal membrane electroosmosis. *J. Pharm. Sci.* **88**:1044–1049 (1999).
19. T. R. Mollee, Y. G. Anissimov, and M. S. Roberts. Periodic electric field enhanced transport through membranes. *J. Membr. Sci.* **278**:290–300 (2006).
20. K. D. Peck, A. H. Ghanem, W. I. Higuchi, and V. Srinivasan. Improved stability of the human epidermal membrane during successive permeability experiments. *Int. J. Pharm.* **98**:141–147 (1993).
21. K. D. Peck, A. H. Ghanem, and W. I. Higuchi. Hindered diffusion of polar molecules through and effective pore radii estimates of intact and ethanol treated human epidermal membrane. *Pharm. Res.* **11**:1306–1314 (1994).
22. A. J. Bard and L. R. Faulkner. *Electrochemical Methods: Fundamentals and Applications*, Wiley & Sons, New York, 1980.
23. H. Zhu, K. D. Peck, S. K. Li, A. H. Ghanem, and W. I. Higuchi. Quantification of pore induction in human epidermal membrane during iontophoresis: the importance of background electrolyte selection. *J. Pharm. Sci.* **90**:932–942 (2001).
24. Y. A. Chizmadzhev, A. V. Indenbom, P. I. Kuzmin, S. V. Galichenko, J. C. Weaver, and R. O. Potts. Electrical properties of skin at moderate voltages: contribution of appendageal macropores. *Biophys. J.* **74** (2 Pt 1) 843–856 (1998).
25. M. E. Johnson, D. Blankschtein, and R. Langer. Evaluation of solute permeation through the stratum corneum: lateral bilayer diffusion as the primary transport mechanism. *J. Pharm. Sci.* **86**:1162–1172 (1997).
26. D. A. van Hal, E. Jeremiasse, H. E. Junginger, F. Spies, and J. A. Bouwstra. Structure of fully hydrated human stratum corneum: a freeze-fracture electron microscopy study. *J. Invest. Dermatol.* **106**:89–95 (1996).
27. R. R. Warner, K. J. Stone, and Y. L. Boissy. Hydration disrupts human stratum corneum ultrastructure. *J. Invest. Dermatol.* **120**:275–284 (2003).